ENERGY ANALYSIS AND PLANT OPERATION OPTIMIZATION OF THE ALUTO LANGANO GEOTHERMAL PLANT RELATED TO PLANT PROBLEMS

Senay Gebregiorgis
Ethiopian Electric Power Corporation - EEPCo
P.O. Box 1233, Addis Ababa
ETHIOPIA
ggsenay@yahoo.com

ABSTRACT

Continuous operation of a geothermal power plant basically relies on the sustainable geothermal source and skilled operation of the resource and power plant. Major problems encountered are mostly related to the chemistry of geothermal water. Aluto Langano pilot plant has encountered many problems over the years of service. This paper discusses some of the plant problems and, in order to gain experience and increase understanding of the operation and maintenance of the plant, gives a review of actions taken to overcome similar problems in other plants. An energy analysis of the plant is made on EES to analyze how the plant reacts to different operating conditions and to optimize operation. As the geothermal field of Aluto Langano is a high-temperature field, silica formation with current flow is also analyzed.

1. INTRODUCTION

Aluto Langano geothermal power plant was constructed by Ormat under a turnkey contract of GENZL (EPC) and has been operational since May 1998. It is the first geothermal power plant in Ethiopia. The power plant is designed to generate a net output power of 7.28 MWe (8.52 MWe gross) with two units. These are:

 i.   A geothermal combined cycle unit (GCCU), a steam turbine integrated with binary turbine that generates 3.9 MWe;
 ii. An Ormat energy converter (OEC) with an output of 4.6 MWe (Ormat, 2001).

There are four production wells from which steam and brine are supplied to the power plant. The production wells are LA-3, LA-4, LA-6 and LA-8 and there is one reinjection well, LA-7. Well LA-3 and LA-6 are high enthalpy wells supplying steam to the GCCU and brine to a flash tank, used as a heat source for heating the isopentane in the OEC unit. Wells LA-4 and LA-8 are low-pressure wells supplying steam to the vaporizer of the OEC unit and brine to the flash tank. Each well has its own steam separator near the wellhead. After some years in operation, many problems were recognized related to production wells and surface equipment.

The main problems visualized are:

- Scaling problems in production and reinjection wells;
- Well head valve trouble;
- Deposition in well pipes;
- Cooling tower problems;
- Steam turbine corrosion;
- Leakage of isopentane in heat exchangers;

Pressure decline after one year in operation and the current conditions are indicated in Table 1. Plant shutdown followed, with the current ongoing rehabilitation of the plant including some modifications of the existing system. The steam turbine was modified to compensate for the decrease in the wellhead pressure. From four stages of the turbine, the two high-pressure sides were removed with an intermediate labyrinth seal and replaced with a balancing weight. Investigative results of the wells and their past chemical content are indicated in Table 2. It can be seen from the logging results in Table 2 that some of the wells have experienced major blockages which cause restriction to flow. The reason for the blockages could be scaling or deposition of sand. Most problems in the plant operating conditions are related to the chemical composition of the geothermal fluid. In this report, causes of scaling and corrosion problems on surface equipment are discussed. Safe operation of the wells with regard to silica saturation is also discussed, as well as operation optimization of the plant with an energy analysis with respect to pressure reduction of the wells.

TABLE 1: Wellhead pressure drop of Aluto Langano wells

	LA-3	LA-4	LA-6	LA-8
Initial pressure (bar	12.5	6.4	13.5	8.4
After one year (bar)	5.0	3.2	6.2	3.0
Current status	Productive	Closed	Productive	Closed

TABLE 2: Production and reinjection well data for the Aluto Langano power plant
(Ketema and Solomon, 1983; Teklemariam et al., 1996)

	LA-3	LA-4	LA-6	LA-8	LA-7
Total depth (m)	2144	2061	2202.8	2500	2448.5
Status of well	Productive	Non- product.	Productive	Non-product.	Active reinjec.
Permeable zone (m)	2000-2121	1445-1800	2000-2200	2300-2500	2100-2300
Chemical composition, gas content and pH values					
SiO_2	573	300	749	479	-
HCO_3	1015	1574	1305	1922	-
Gas (% by total mass)	2.3	2.1	2.6	1.5	-
pH	7.4	9.0	8.7	9.2	-
Logging result in July 1996 (Benoit, 2006)					
8.2" go devil depth (m)	-	-	-	-	648
7" go devil depth (m)	-	-	152	103	-
5.7" go devil depth (m)	-	1080	1898	1911	1525
4.5" go devil depth (m)	-	2029	2183	-	-
Logging result May 2006 (Benoit, 2006)					
6" go devil depth (m)	977	745	-	103	1142
4.5" sinker bar depth (m)	2138	1060	1835	-	1461.7
3" pipe depth (m)	-	1085	-	701	-
1.75" sinker bar depth (m)	-	2000	2170	-	-
1.3" sinker bar depth (m)	2125	2035	2178	702	1461.7

2. ENERGY ANALYSIS OF THE PLANT

2.1 Plant flow stream

The steam field includes two high-temperature wells (LA-3 and LA-6) and two medium-temperature wells (LA-4 and LA-8). The current working pressure of the high-temperature wells ranges from five to six bars. There are four steam separators, one for each well. From the high-temperature wells, the separated steam goes to the back pressure turbine at the GCCU unit (geothermal combined cycle unit). The back-pressure steam passes through the isopentane vaporizer. The condensed brine from the vaporizer is re-injected after passing through the pre-heater.
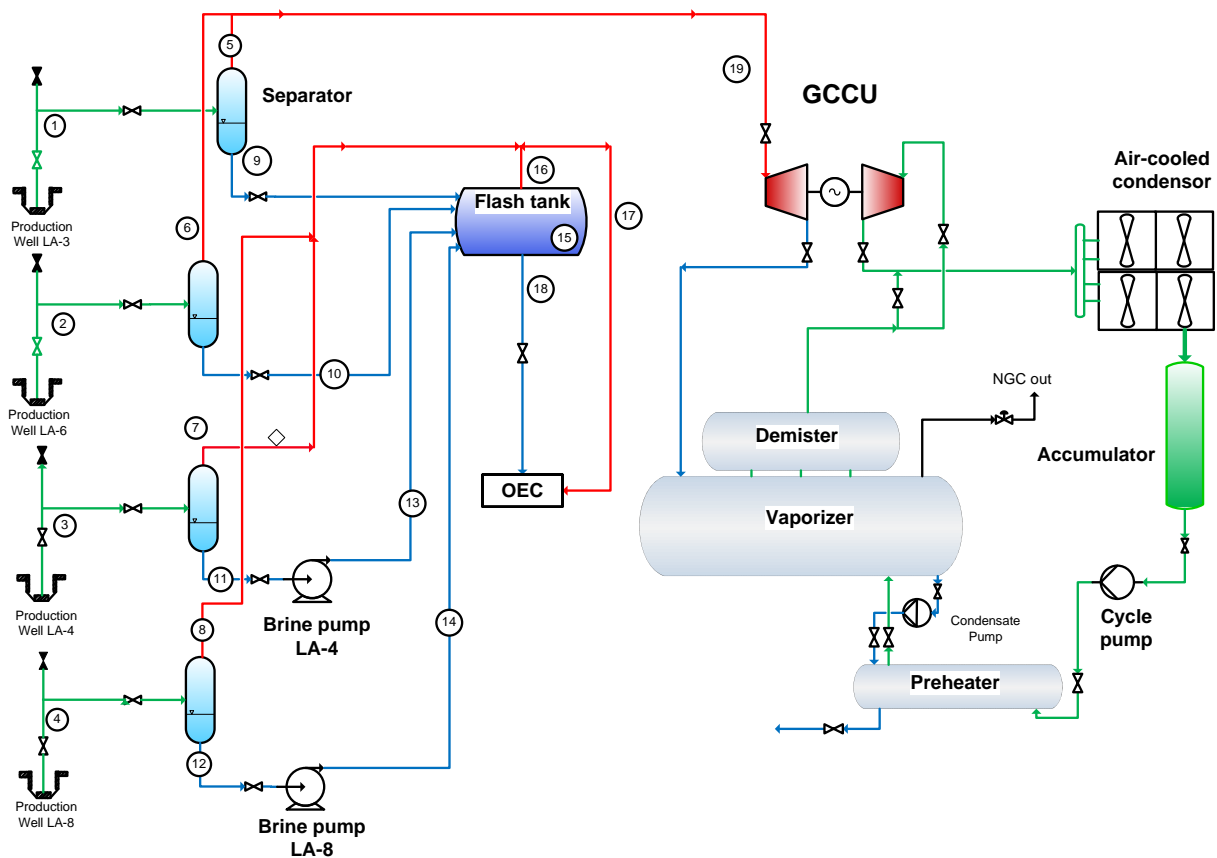
FIGURE 1: Aluto Langano GCCU flow diagram

The brine from all wellhead separators is flashed in the medium-pressure separator operating at 5 bars. The brine from the flash tank then heats the isopentane in the cascaded pre-heaters of OEC unit (Ormat energy convertor unit) before reinjection. The steam from the flash tank is mixed with the steam from the two low-temperature wells. This mixed steam is condensed passing through the isopentane vaporizer of the OEC unit. After condensing in the vaporizer, it is mixed with the brine from the flash tank for further use in the pre-heaters. After cooling in the condenser, the isopentane is pressurized with two cycle pumps and pumped to a recuperator and to a pre-heater. The preheated isopentane is vaporized in the vaporizer with steam from the flash tank before expanding in the two cascaded high and low pressure turbines.

There are two isopentane cycles working independently for the GCCU and OEC units. The isopentane cycle is explained by a Rankine cycle. Heat is added to the working fluid at constant pressure at about six bars in the heat exchangers, in the vaporizer and in the pre-heater, followed with isentropic expansion in the turbine. The condensers receive the gas from the turbine, the heat is removed with fan air coolers, and the gas is condensed into a liquid. The cycle repeats with pumping of the isopentane to the preheater.
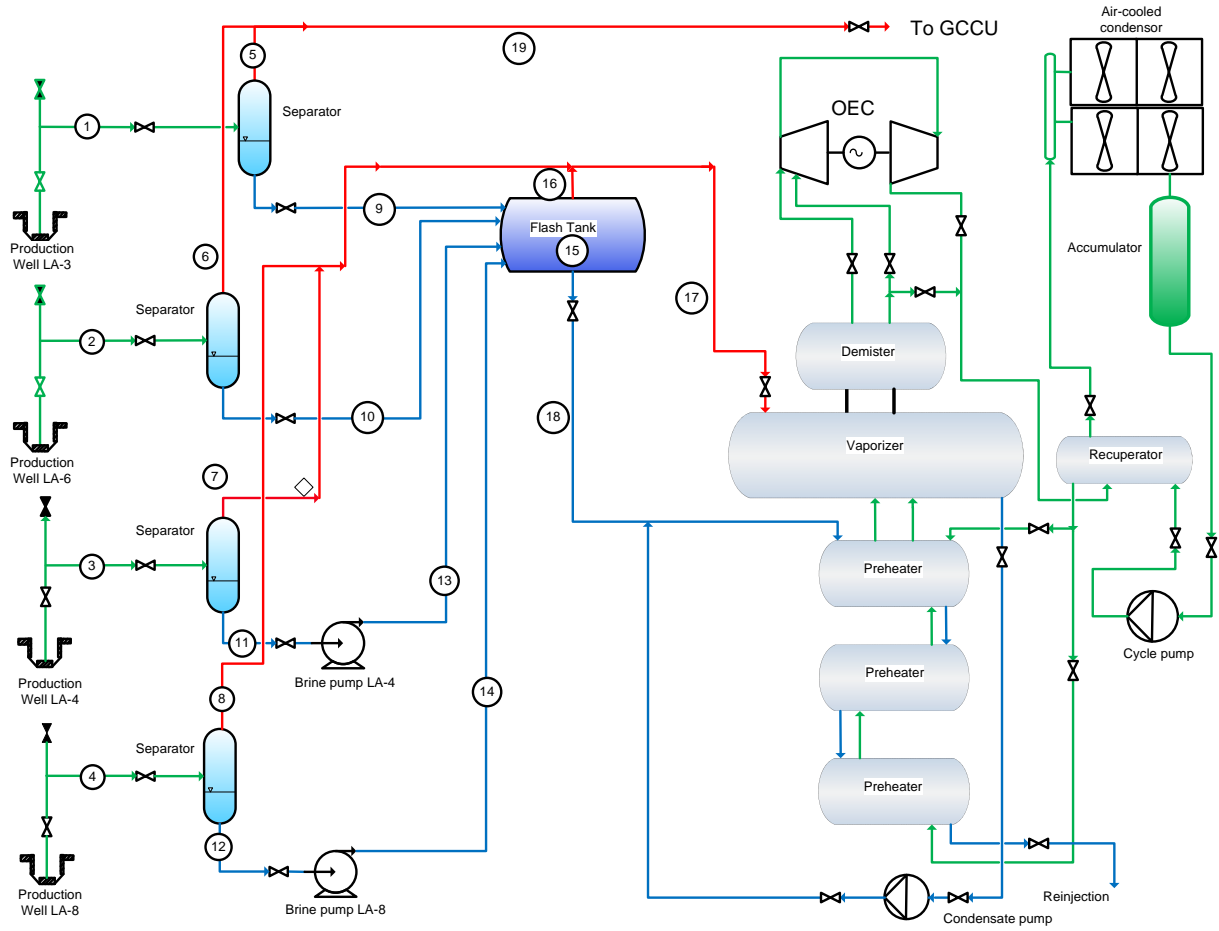
FIGURE 2: Aluto Langano OEC flow diagram

2.2 Steam separator

The geothermal fluid from the wells is a two-phase fluid. The steam must be separated before it goes to the back-pressure turbine. The separation process is an isobaric process. The steam that exits the separator is piped to a demister before it enters the steam turbine.

The steam fraction is calculated from mass balance and energy balance in the separator. Mass balance of the flow is given as:

$$\dot{m}_1 = \dot{m}_2 + \dot{m}_3$$

where $\dot{m}_1$ = Total mass flow from the production well (kg/s);
$\dot{m}_2$ = Mass flow of steam (kg/s);
$\dot{m}_3$ = Mass flow of water (kg/s).

Energy balance of the flow is:

$$\dot{m}_1 h_1 = \dot{m}_2 h_2 + \dot{m}_3 h_3$$

where h_1, h_2, h_3 are enthalpy values (kJ/kg) corresponding to the mass flows.

The steam mass fraction in the separator x_1 is:

$$x_1 = \frac{h_1 - h_3}{h_2 - h_3}$$

2.3 Steam transmission

After the steam is separated it is transmitted to the plant station. The steam mass flow is:

$$\dot{m} = \rho_s v_s \left(\frac{\pi D_s^2}{4}\right)$$

where v_s = Velocity of steam (kg/s);
          ρ_s = Density of steam (kg/m³);
          D_s = Inner diameter of steam pipe (m).

The pressure drop, as the steam flows from the separator station to the power plant, is calculated as follows (Cengel and Turner, 2001):

$$\Delta p = \rho_s g (\Delta z + h_L) 10^{-5}$$

where Δz = Difference in elevation between the separator location and the power plant (m);
          h_L = Friction head loss (m).

The friction head loss comes from the Darcy equation:

$$h_L = f \frac{L_e \, v_s^{\,2}}{D_s \, 2g}$$

where f = Friction factor;
          L_e = Equivalent length (m).

The equivalent length, L_e, is given as:

$$L_e = L_p + \sum h_i n_i D_i$$

where L_p = Length of pipe (m);
          h_i = Equivalent length factor (m);
          D_i = Inner diameter (m);
          n_i = Number of valves, bends and connections.

The friction factor for turbulent flow in smooth as well as rough pipes is calculated from the Colebrook equation:

$$\frac{1}{\sqrt{f}} = -2 \log \frac{\varepsilon/D_s}{3.7} + \frac{2.51}{Re\sqrt{f}}$$

where ε = Surface roughness (m);

The Reynolds number (Re) corresponding to the flow and the pipe is:

$$Re = \rho_s v_s \frac{D_s}{\mu_s}$$

where μ_s = Coefficient of dynamic fluid viscosity (Nsm⁻²).

2.4 Expansion in the turbine

The plant includes two kinds of axial turbines, for steam and isopentane. The steam turbine on the GCCU unit uses steam from the separator of the two high-temperature wells. One organic turbine is installed on the GCCU unit which gets its heat source from the back pressure steam of the steam turbine on the GCCU (see Figure 1).

The expansion process in the turbine starts with the saturated steam and expands isentropically. The OEC unit has two organic turbines working in series (see Figure 2). The expansion of isopentane is completed in the superheated state. The efficiency of the entire turbine is greater than for individual stages. This is explained with the Mollier chart. As the constant pressure lines diverge, the isentropic enthalpy drops charged to a turbine stage are greater than for the entire turbine (El-Wakil, 1984) (see Figure 3).
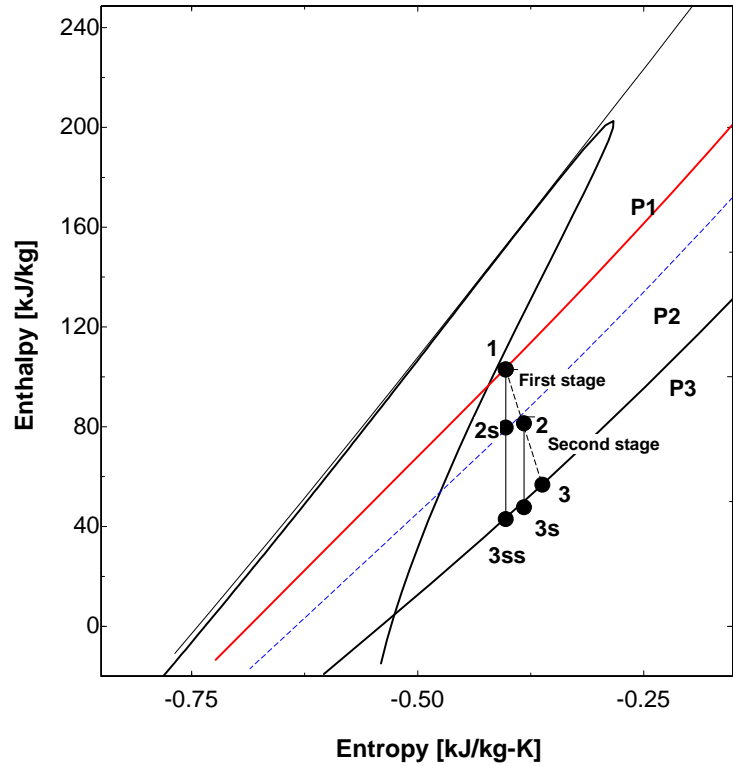
FIGURE 3: Isopentane expansion in turbine

Efficiency of the two stages is:

$$\eta = \frac{h_1 - h_3}{h_1 - h_{3ss}}$$

And it is greater than the efficiency of one stage:

$$\eta = \frac{h_2 - h_3}{h_2 - h_{3s}}$$

where h_1 and h_2 are enthalpy values (kJ/kg) at the inlet and the outlet of the first stage;
h_3, h_{3s} and h_{3ss} are enthalpy values at the outlet of the turbine (Figure 3).

The electrical power W (kW) out of the turbines is calculated as:

$$W = \dot{m}(h_3 - h_1)\eta_\mathrm{g}$$

where $\dot{m}$ = Flow rate (kg/s);
η_g = Generator efficiency.

2.5 Heat exchanger

The heat exchangers mentioned here are of shell and tube type where the hot brine or steam passes through the tube side and the isopentane passes through the shell side. This works for the pre-heaters and vaporizers installed for GCCU and OEC units. The outlet temperature of the working fluid and

the brine is calculated from the inlet enthalpies and the existing area and overall heat transfer coefficient of the heat exchangers in EES, with:

$$\dot{Q} = \dot{m}_H\left(h_{H,in} - h_{H,out}\right) = \dot{m}_c\left(h_{c,out} - h_{C,in}\right)$$

$$\dot{Q} = UA \times LMTD$$

where $\dot{Q}$ = Heat transferred in heat exchanger (kJ);
U = Overall heat transfer coefficient (kJ/m^2°C);
A = Heat transfer area (m^2); and
LMTD = Logarithmic mean temperature difference (°C).

LMTD is calculated as follows:

$$LMTD = \frac{(GTTD) - (LTTD)}{ln\left(\frac{GTTD}{LTTD}\right)}$$

where *GTTD* = Greater terminal temperature difference, $T_{H,in}$-$T_{C,out}$;
LTTD = Lower terminal temperature difference, $T_{H,out}$-$T_{C,in.}$

2.6 Air cooled condenser

The isopentane circulating in the system is condensed in the cooling towers. The types of cooling towers installed are the dry type for both units. A dry cooling tower is one in which the circulating fluid passes through finned tubes over which fan-forced cooling air passes. All heat rejected from circulating isopentane is in the form of sensible heat to the cooling air.

The exhaust isopentane from the organic turbines enters the condenser in a superheated state (3) and is condensed to saturated liquid (4), shown in Figure 4. The condensed isopentane is collected in the isopentane accumulation tank for further recirculation. In the case of the OEC unit, the exhaust isopentane from the turbine enters the recuperator where it is cooled before it enters the condenser, still in a superheated state.
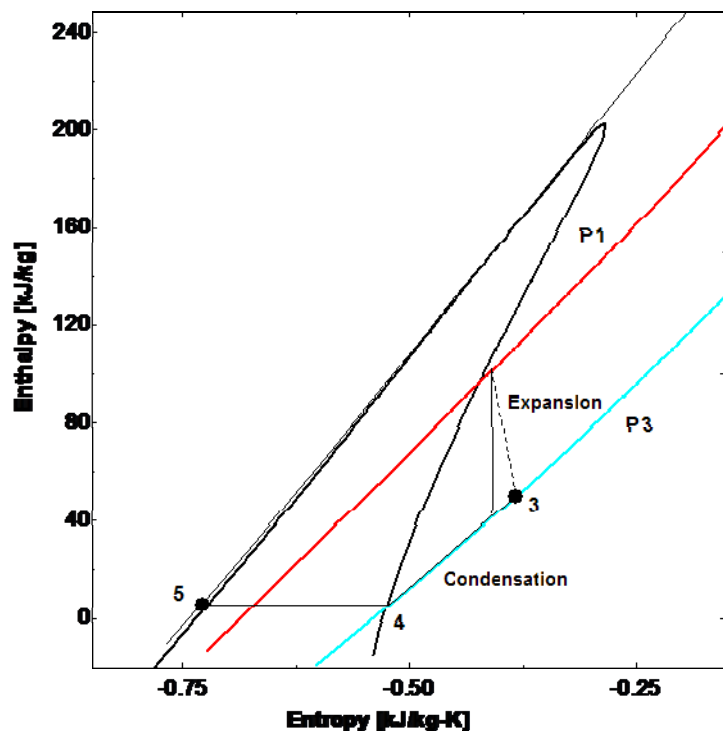
FIGURE 4: Isopentane condensation in the cooling tower

2.7 Non-condensable gas extraction

The steam entering the turbine contains gas such as CO_2, and H_2S. The mixture of gases entering the turbine is homogeneous. This mixture is made to flow through a turbine in which the work of the turbine is produced by the joint expansion of vapour and non-condensable gases. Along the path of

expansion the steam will partly condense and in the condenser two phases will evolve:. the liquid phase in which the dissolved gas constitutes a negligible quantity, and an equilibrium mixture of water vapour and gas. The gas is released after primary condensation in the vaporizer. This gas, after initial compression and partial cooling in the vaporizer, must be compressed again before it can be rejected to the atmosphere. Compression can occur by means of an ejector which is intrinsically inefficient, or through a rotary compressor. There is no need to compress the gas if the condensation is at or above atmospheric pressure.

2.8 Pumps

The following equations are used to calculate the outlet pressure of the pump:

$$\dot{W}_{pump,shaft} = \eta_{motor}\, \dot{W}_{electric}$$

$$\dot{V}\, \Delta p = \eta_{pump}\dot{W}_{pump,shaft}$$

$$\dot{V} = \frac{\dot{m}}{\rho_{water}}$$

where Δp = Pressure gain (bar);
  $\dot{V}$ = Volume flowrate (m^3/s);
  $\dot{m}$ = Mass flowrate (kg/s);
  η_{pump} and η_{motor} = Efficiency of pump and motor of the pump;
  $\dot{W}_{pump,shaft}$ and $\dot{W}_{electric}$ = Electric power of motor and power delivered to the pump, respectively (kW).

3. EES MODEL

The Engineering Equation Solver program – EES (F-Chart Software, 2004) was applied for the analysis. It is used for calculating silica saturation limits with empirical formulas and for energy analysis of the plant. The EES model for silica saturation is done with silica concentration from downhole samples and reservoir temperature values from the past data. The values used in the calculation are stated in Table 3. The energy analysis was done with pressure vs. flow and enthalpy vs. pressure data taken from the past (Figures 5 and 6) (Amdeberhan, 2006).

TABLE 3: Aluto Langano downhole silica concentration and temperature

	LA-3	**LA-4**	**LA-6**	**LA-8**
Silica concentration (ppm)	556	317	558	418
Temperature (°C)	315	235	335	265

An energy analysis model was done in EES. Part of the model was done as follows:

- The model starts from the four wells LA-3, LA-6, LA-4, and LA-8;
- Energy and mass balance analyses were done for steam separation at separators;
- Energy and mass balance analyses were also done for steam and water separation in the flash tanks;
- Pressure drop calculations were done for the separated steam from the high-pressure separators for LA-3 and LA-6 to the connection point, where the two lines connect;
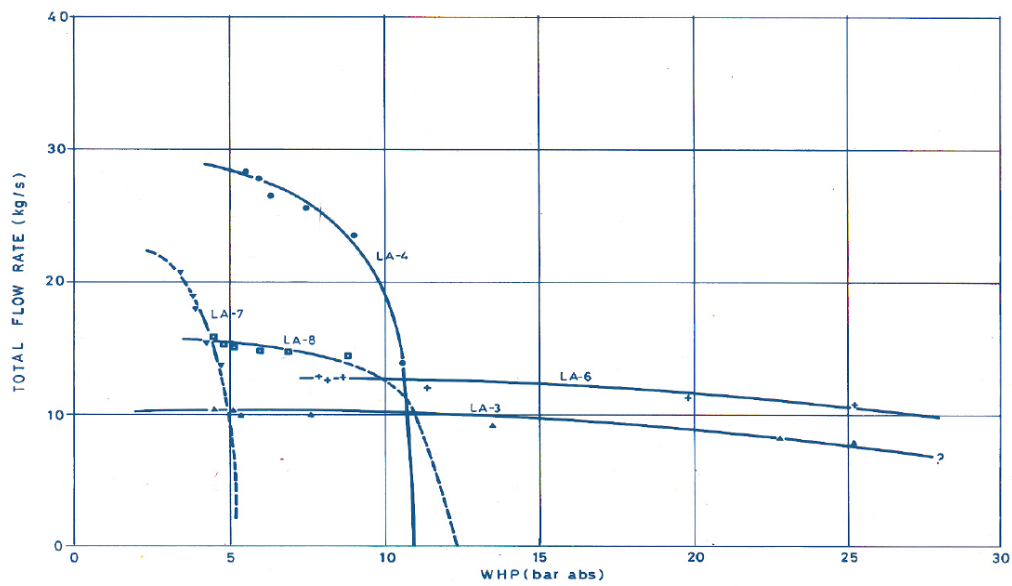- Pressure balancing was done to operate the two wells in parallel;

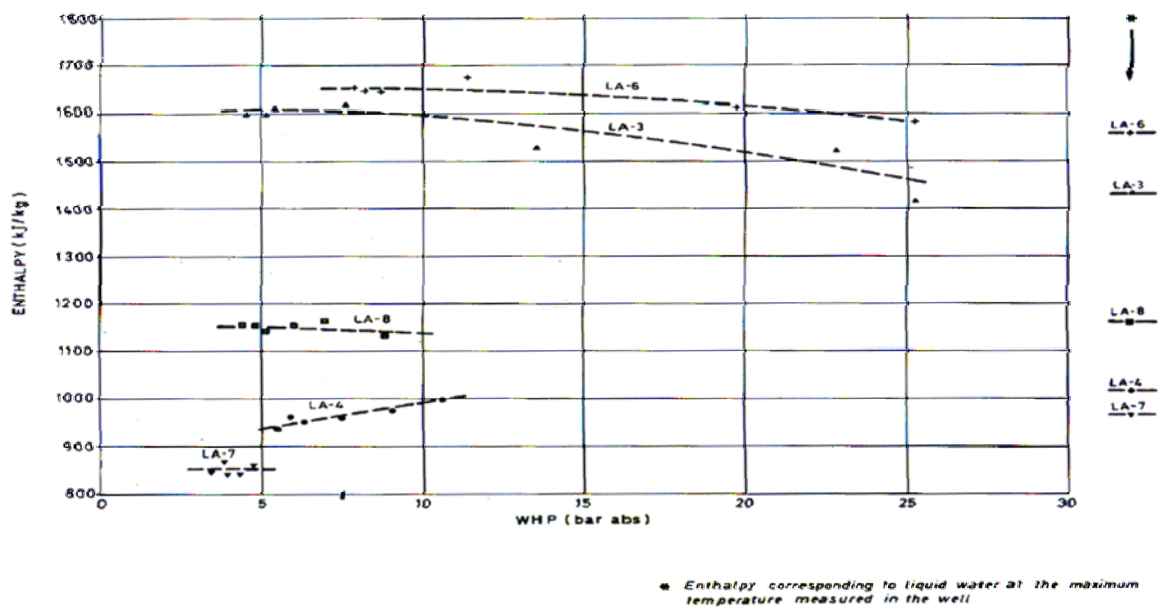FIGURE 5: Aluto Langano output characteristics

FIGURE 6: Aluto Langano, flow of wells vs. wellhead pressure

- Pressure drop calculations were also done for the steam pipeline from the connection point to the GCCU steam turbine and considers superheating of the steam before it gets in to the turbine;
- Power generated was calculated with steam expansion in the turbine;
- Maximum heat transferred in the vaporizer was calculated with consideration of minimum pinch.
- Power generated was calculated with isopentane expansion in the organic turbine.

An analysis of heat transfer from the steam to the isopentane was calculated for three possible cases:

Case one: Steam leaves the vaporizer without full condensation, i.e. there is steam left at the vaporizer exhaust (Figure 7).

Case two: Heat gained by the isopentane to the bubble point is less than the heat released by the steam from the bubble point to the outlet (Figure 8).

Case three: Heat gained by the isopentane to the bubble point is greater than the heat released by the steam from the bubble point to the outlet (Figure 9).

As the superheated temperature of the isopentane from the vaporizer outlet increases, the work gained from the expansion in turbine increases. The following assumptions were made on data used with the energy analysis of the plant:

- Non-condensable gas content from LA-3 and LA-6 is 2.3 and 2.6, respectively ;
- The efficiency of brine pumps at wellhead stations 4 and 8 is 0.85;
- The isentropic efficiency of the steam turbine is 0.86;
- The isentropic efficiency of the organic turbine is 0.86;
- The heat transfer coefficient of the vaporizer is 1.4;
- The heat transfer coefficient of the pre-heater is 0.8.
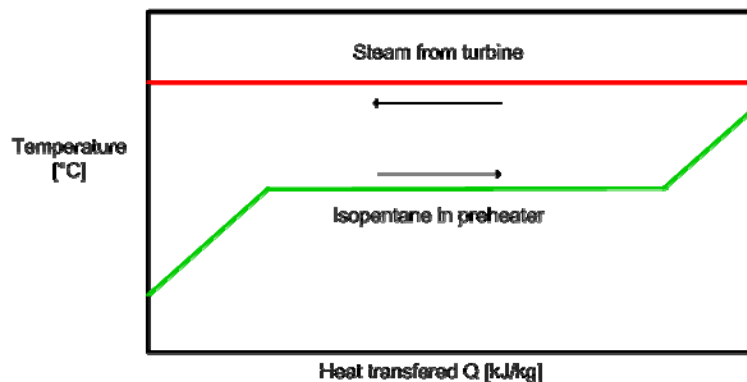
FIGURE 7: Flow in vaporizer, case one
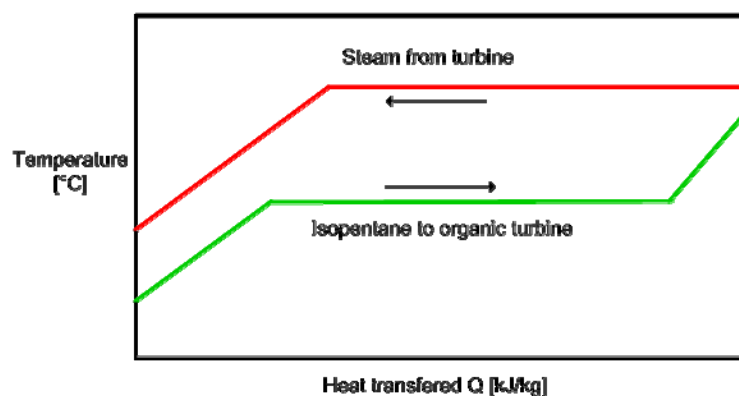
FIGURE 8: Flow in vaporizer, case two
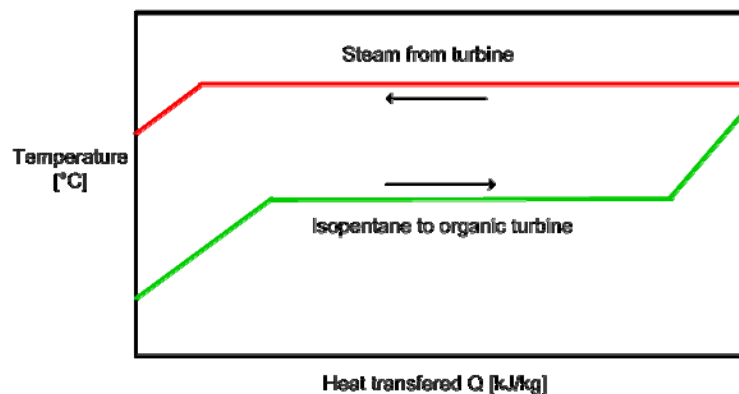
FIGURE 9: Flow in vaporizer, case three

4. SAFE PLANT OPERATIONS, START UP AND STOP

This part of the report discusses safe operation of the power plant. The operation of the binary system starts with filling of isopentane. Initially, the isopentane system has to be cleared of oxygen using non-reacting gas, nitrogen or with a vacuum pump as experienced in Aluto Langano. Filling the system with isopentane is accomplished by venting the nitrogen and opening the isopentane inlet valve from the storage tank to the system. As the isopentane is heavier than nitrogen, the nitrogen is pushed out of the system. The nitrogen and vapour isopentane are vented at the top of the radiators and high points while liquid isopentane is added from the bottom. When equilibrium pressure is reached between the storage tank and the system, a make-up pump starts to fill the system with pressure. The evaporator has to be filled to 70% of the volume and the turbine is bypassed with a bypass valve connection.

After all the necessary auxiliary and electrical systems have been started, a small amount of brine from the wells is circulated to heat up the isopentane in the pre-heaters. The isopentane vapour in the evaporators is made to circulate through the bypass valve. When the required temperature has been reached, the steam turbine and the organic turbine are automatically started simultaneously.

The bearings on the GCCU and OEC units are supplied with pressurized lubricating oil. The lubricating pumps must be started before starting the turbine and stopped after the turbine has shut down. In case of power failure and sudden shut down of turbines, the electric motor driven pumps are substituted with air diaphragm pumps, so it is important to check the automatic operation of the pumps that are in operation, to prevent damage to the bearings.

In case of planned or forced plant shut down, the following precautionary guidelines will aid in preparing the plant for its next start-up (Morris and Stephens, 1981):

- Steam flow at the power plant inlet should not be shut off too rapidly, otherwise physical damage of gathering systems will occur; this is done automatically.
- Steam flow at the wellheads should not be closed off completely (well shut-in), and cycling of temperature and pressure within the wells should be minimized. If care is not exercised, the integrity of the well casing and the exposed walls of the wells may be jeopardized.
- Steam flow and pipe line temperature should be maintained at appropriate levels (usually 35% of full flow) to prevent condensation build-up in the steam gathering system. If condensation takes place, then upon power plant start-up, slugs of condensate will have to be drained from the system to avoid damage to the pipelines and turbine.

If the power plant has to be shut down for a long time the turbine, vaporizers and the pre-heaters on the brine side must be drained and vented and kept dry.

5. PLANT COMPONENTS

5.1 Main bearings

The two principal types of bearings in steam turbines are (1) the main bearing, which carries the weight of the rotor and which also prevents any excessive movement of the rotor in any direction perpendicular to its axis and (2) the thrust bearings, which restrain the rotor from excessive movement in either direction parallel to the axis of the rotor. The common main bearings are plain bearings and ball bearings. The plain bearings generally consist of a Babbitt which contains oil grooves and a lining held in place by a spherical seat. The lining is

FIGURE 10: Aluto Langano GCCU steam turbine bearing damage

usually split in two along the horizontal centre line, which are called the upper lining and the lower lining. The lining is supported with a pedestal seat and covered with a bearing cover.
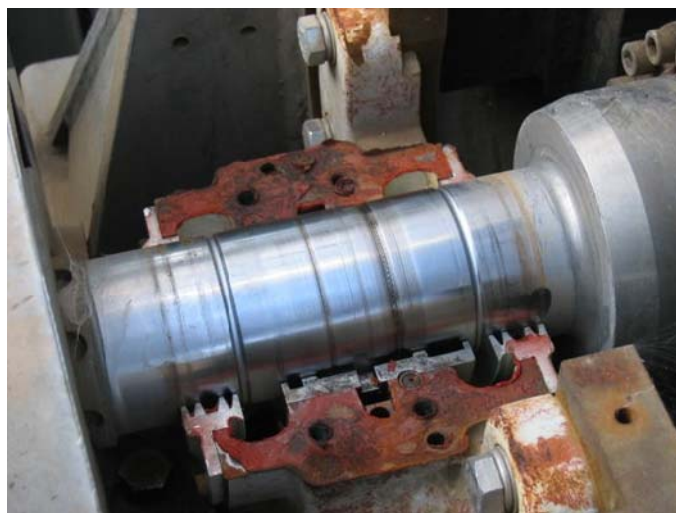
In the Aluto Langano single-flash turbine, plain bearings are used and for the ORC turbines, ball bearings are used. Care for the turbine bearings mainly includes proper lubrication and alignment. If proper lubrication is not maintained, excessive wear of the bearings will result, or the bearings may be burned out. This happened on the single flash turbine at the Aluto plant (Figure 10). If slight

misalignment due to wear is discovered, it may be corrected by removing and inserting shims. Excessive wear in the bottom of the bearing lining usually results in one of the following conditions:

1. Misalignment of the bearing;
2. Shoulders along oil grove, which will cut off lubrication and cause heating;
3. Contact between some stationery and some rotating parts of the turbine;
4. Hard parts of the Babbitt wearing the journal irregularly; and
5. Excessive clearance in the upper half of the liner, which may permit the oil to go through causing a lack of lubrication.

Obviously, the remedy here is to install a new lining or to re-Babbitt the old lining.

5.2 Shaft seal

Sealing is used to minimize the leakage of steam or hydrocarbons to the outside air, or air to the inside of the casing through the clearance between the rotating and stationery parts. The type of sealing method discussed here is a metallic labyrinth gland which is widely used. It has two kinds of applications. The first one is the single-labyrinth gland which consists of an annular saw tooth facing the smooth shaft. The second one is double-labyrinth gland which consists of annular rings on a rotating shaft which fits into the annular of the labyrinth gland.

The advantage of a double-labyrinth gland is that there are no rubbing surfaces. Therefore, it is frictionless and consequently has a long life, but it can limit the axial play of the shaft. Of course the steam has to be clean enough so scales will not grind down the shaft as shown in Figure 11.

For the steam turbine in Aluto Langano, a double-labyrinth gland is applied and for the organic turbine, a double mechanical seal is applied.

FIGURE 11: Aluto Langano GCCU labyrinth seal damage

5.3 Leak detection method

If brine leaks in small amounts to the hydrocarbon system stream, the fluid combination becomes corrosive and can result in pitting on the hydrocarbon side of the heat exchanger tubes. Also, if brine is present in the hydrocarbon, it can cause turbine damage by condensing inside the turbine. Consequently, the detection of brine in the hydrocarbon is essential to maintain reliable long-term operation.

The need to install leak detectors at the heat exchangers is important as heat exchangers at the Aluto Langano binary cycle plant failed due to pitting corrosion after less than three years operation. Decrease of the hydrocarbon volume indicated major leakage in the heat exchanger. In the investigation, many leaks were found at the heat exchanger tubes. Ordinary corrosion measuring instruments detect only uniform corrosion rates. Pits in heat exchanger tubes can penetrate the wall long before the bulk of the tube is seriously corroded. When pits do develop, hydrocarbon will be lost to the brine. Under ordinary operating conditions, hydrocarbon pressure in a binary plant will exceed

both the brine pressures. But at the starting and stopping of the plant, it could be vice versa. Early detection of any hydrocarbon leaks can save maintenance time and maintenance cost. If leaking tubes are found, further leakage can be prevented by plugging the ends. Available leak detectors to detect brine leak to the hydrocarbon or the hydrocarbon to the brine are stated below (Robertus et al., 1984).

5.4 Organic fluid leak detection method

Leaks to the brine cause it to become contaminated and possibly unacceptable for reinjection. The following detector system works by continuously sampling the brine stream at a very small rate (Figure 12). It can detect the presence of hydrocarbons in brine streams down to 2 ppm liquid hydrocarbon in the brine. The unit first cools the liquid stream and then reduces the pressure in an expansion chamber around atmospheric pressure so the hydrocarbon vaporizes. The brine has inherent gases like CO_2, which sweep out the hydrocarbon into the gas phase, and permits good sensitivity to the non-dispersive infrared analyzer (NDIR). For example, if a brine contains 500 ppm non-condensable gas and a leak were contributing 1 part per million (ppm) into the working fluid, the off-gas from this brine could consist of ~0.2% (~2,000 ppm) leaked working fluid.
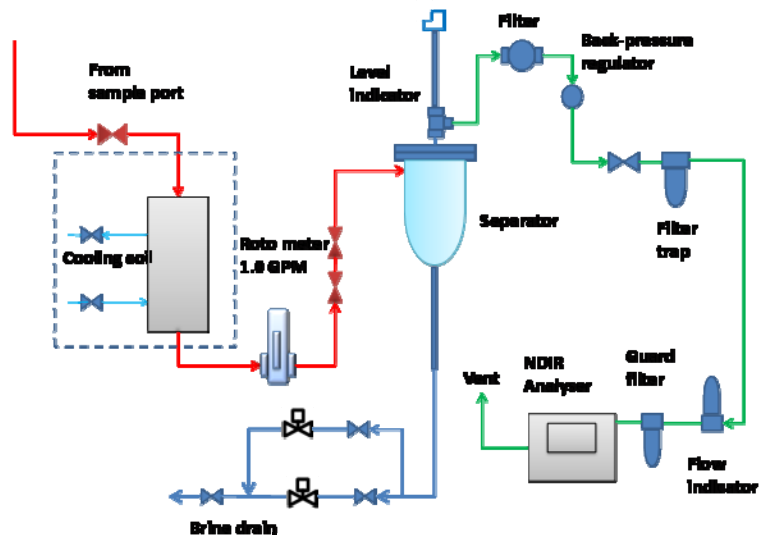
FIGURE 12: Organic fluid leak detection system

5.5 Brine into organic fluid leak detector

Under ordinary operating conditions, hydrocarbon pressure in a binary plant will exceed both the brine and cooling water pressures. Consequently, leaking heat exchanger tubes should result in hydrocarbon contamination of either the brine or cooling water. Past experience, however, has shown that the hydrocarbon fluid can be contaminated with brine or cooling water, especially during start-up and shutdown of the plant.

The unit continuously samples a hydrocarbon stream. The hydrocarbon is cooled and flows to a settling chamber which greatly reduces its velocity. If any water or brine is present, the aqueous phase will drop to the bottom of the settling chamber because it has higher density than the hydrocarbon. The presence of the aqueous phase is detected by a capacitance probe. As the settling chamber fills with water, the probe produces higher and higher voltage. The unit (Figure 13) is designed to be self emptying so the size of the leak can be related to the number of fill frequency.

5.6 Air cooled condenser

In air cooled condensers, the temperature of the air that comes out of the tower in order to cool the working fluid in the condenser is around 25°C. Typical values range from 20 to 30°C resulting in a working fluid temperature from 40 to 50°C. In air cooled condensers, no water supply is necessary. The circulating air is forced to pass through the fins of the radiator with electrical motor driven fans. Air cooled condensers do not require any amount of chemical additives or periodic cleaning as do wet

towers. Due to the need for a many times higher heat exchange surface and a large volume of air that has to be moved through them, they are considered an expensive option.

In Aluto Langano there are 39 installed fans. Most of the fans used to fail frequently with belt hardening and bearing failure, which are related problems. In order to achieve better reliability, improvements in design should be made. Practical experience can be gotten from the Svartsengi power plant. In Svartsengi, the fan belts hardened because of hydrogen sulphide in the atmosphere and high humidity. This problem was solved by installing geared electrical motors for the fans (Thórólfsson, 2005) (Figure 14).

FIGURE 13: Brine leak detection system

5.7 Corrosion prevention, turbine and heat exchanger

Geothermal steam contains corrosive gases and dissolved gases. Before discussing the prevention of corrosion it is good to know the types of corrosion. Dissolved minerals undergo ionic dissociation in the brines, and contribute to their salinity, chlorinity, and electrical conductivity; altering their pH increases their corrosivity. Dissolved corrosive gases are oxygen, carbon dioxide, ammonia (NH_3) and hydrogen sulphide.

Corrosion is a natural process of deterioration of metal in a corrosive environment. The most frequently occurring types of corrosion are (Koutsoukos and Andritsos, 2002),

FIGURE 14: Svartsengi plant modified gear coupled cooling fan

- *General corrosion* is the wasting away of a metal in a corrosive environment, resulting in an actual decrease in thickness of the original metallic structure. The wasting away occurs relatively uniformly over the surface exposed to the corrosive environment.
- *Pitting* is a form of localized corrosion in which a small portion of a metallic structure is corroded at a rate much faster than that of the bulk of the structure. If proper material is not used, unexpected failures occur due to pitting.
- *Crevice corrosion* is a localized form of corrosion. It is an accelerated attack observed at a junction between metals exposed to a corrosive environment.
- *Galvanic corrosion* is caused when dissimilar metals are connected in an electrolyte solution. Under proper conditions, one metal will experience accelerated corrosion. The alloy highest in the galvanic series will corrode faster.
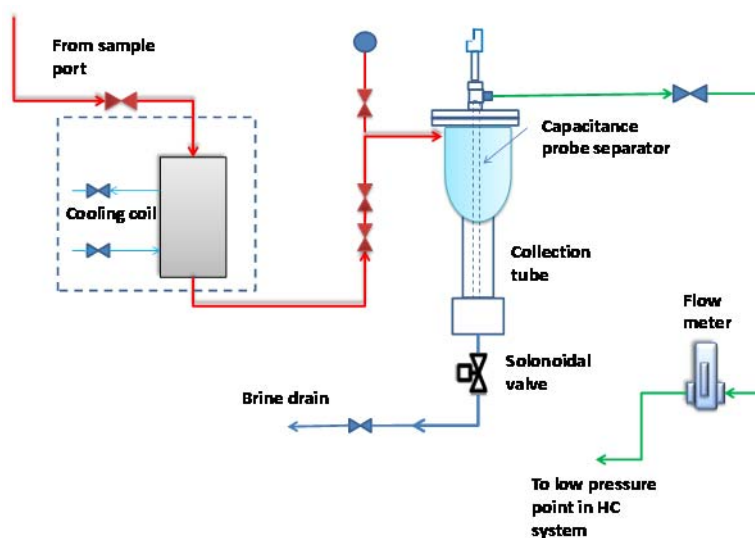
- *Stress corrosion* is a type of corrosive attack which occurs through the combined action of stress and a corrosive environment. The stress can be applied or residual, but it is always tensile stress. In a very corrosive environment cracking may occur at much lower stress levels.

The geothermal steam contains gases like H_2S and impurities such as Cl and so the turbine rotor is exposed to a corrosive environment as well as centrifugal stress which can cause stress corrosion cracking (SCC). The corrosion dominant factors are salinity and the concentration of dissolved oxygen. Salinity influences the brine's electrical conductivity; the chloride (Cl) ion also affects the oxide layer, penetrating the passive film. It can initiate pitting and crevice corrosion at localized sites. Corrosive agents in the geothermal brine can be put in the following way (Valdez et al., 2006)

Hydrogen sulphide (H_2S) is a redundant, toxic and corrosive compound, which originates from well hydrothermal pyrites by natural acidification. It corrodes steel and ductile iron through:

$$Fe+ H_2S \longrightarrow FeS+H_2$$
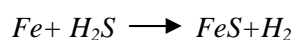
forming a suspension and/or deposits of black iron sulphide, typical of sulphide attack.

Oxygen corrosion of active metals, e.g. iron and steel, depends on the concentration of dissolved oxygen, producing rusted surfaces, through:

$$2Fe+3H_2O+1.5O_2 \longrightarrow Fe_2O_3+ 3H_2O$$
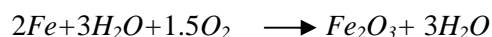
H_2S can function as an oxygen scavenger, thus preventing corrosion in steel. H_2S in the atmosphere corrodes copper.

Carbon dioxide (CO_2) is generated by thermal and/or acidic decomposition of the brine carbonates and bicarbonates, reducing its pH value. A decrease in pH will increase corrosion.
Ammonia NH_3 gas is generated by the chemical decomposition of compounds containing nitrogen such as kerogen (a mixture of organic chemical compounds that makes up a portion of organic matter in sedimentary rocks). Ammonia and its ammonium salt corrode copper alloys, such as the brass and bronze moving parts of well pumps.

TABLE 4: Characteristics of geothermal steam and counter measures

Item	Problem	Counter measure
Wet steam	Moisture impact erosion of moving blades Wetness loss	Installation of drain catcher and erosion protection on turbine blades
Corrosive gas and impurity	Corrosion of turbine parts Stress corrosion cracking of turbine parts	Corrosion resistant material SCC-resistant material
Non-condensable gas	Increase of turbine exhaust pressure	Installation of gas extraction
Scale	Solid particle erosion (SPE) Scale deposition Decreased turbine output	SPE-resistant design and material Installation of separator Large profile steam path design Washing operation Periodic overhaul

Geothermal steam turbines are operated continuously and are simultaneously exposed to corrosive gases which can cause decreases in the output of the turbine and turbine damage. Some counter measures are discussed in Table 4 (Sakuma et al., 2006).
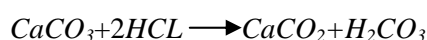
6. SCALE REMOVAL

Scaling is an obstacle in efficient energy recovery from geothermal fields. A major area of concern in power plant operations is scale formations in downhole wells, piping system, flash tank, injection line and other system components. The geothermal scale formation is the result of a high concentration of minerals in geothermal fluid depositing in pipe walls due to flashing and temperature decrease. The scale initiates in the down hole geothermal well and continues throughout the system.

Silica and calcite scaling are considered to be the most common problems in production and reinjection well management. Solubility of calcite increases with a decrease in temperature of brine so calcite scaling is prominent in production wells rather than reinjection wells. Silica has the reverse property, i.e. silica scaling is dangerous in reinjection wells and surface equipment.

There are different types of scale removing methods. Selections of methods are dependent on the cost of the method and the required time, especially if the plant has to be out of operation.

6.1 Chemical removal method

Chemical methods include the use of either acid (acidizing) or base to dissolve an existing scale. The chemical cleaning method has some advantages over the mechanical cleaning method. One advantage is that the pipes or other equipment do not need to be disassembled and reassembled. Acid removes most deposits from the surface. The choice of the acid mainly depends on the type of deposit, price and the strength of the acid. It also depends on the solubility of the salt formed with the reaction, e.g. for $CaCO_3$ deposits:

$$CaCO_3 + 2HCL \longrightarrow CaCO_2 + H_2CO_3$$

The chemicals used for scale removal have to be in a safe concentration for the plant. Some acids are best suited for dissolving a particular type of scale. Based on experience from Salton sea geothermal field (Deutscher, 1980), for scales consisting predominately of amorphous silica, hot NaOH is effective. NaOH in combination with EDTA (Ethylene Diamine Tetra-acetic Acid), was more effective than NaOH alone. A NaOH and NaOH-EDTA combination had little or no effect on PbS or iron rich scales. However, a HCL combination with H_2O_2 or HNO_3 was found effective.

6.2 Mechanical removal method

Mechanical cleaning includes scraping and scratching to clean scale deposits from the walls or casing of a well and from pipe lines. In a well, a scratcher or reamer is lowered into the bore and deposits are removed by the simultaneous rotary transverse motion of the reamer. Reaming is an expensive method for scale removal.

Scraping can be used to remove scale formed in pipe lines by running scrapers through the lines at regular time intervals; these are inserted and removed at inlet and outlet traps. These scrapers, frequently used in saltwater gathering systems, are variously called steel balls, chained rubber balls, plugs, and wire brushes, go-devils, and spiral brush pigs.

6.3 Hydro blasting and cavitation method

Application of a water jet to remove scale may be a potential method for geothermal systems. The Cavitation scale removal method employs pulsating high pressure jets of water which are directed against the scale surface (Figure 15). If, due to low irregularities, the conditions of the water velocity are such that repetitive low- and high-pressure areas are developed, bubbles form and collapse at the

solid-liquid interface. The collapse of these bubbles or cavities results in high shock pressures. The resulting impact tears the scale adhering to the equipment.

In summary, removal of scales from pipe and system components can be done using different methods. Different methods have advantages and disadvantages according to the application. A summarization of typical treatment methods for different applications is given in Table 5 (Phillips et al., 1977).

FIGURE 15: Hydro blast scale removal, Svartsengi power plant

TABLE 5: Typical treatment methods for scale removal

Scale type	Treatment method	Comments
$CaCO_3$ (Calcite) in borehole	Pump inhibited HCL into the well	Acidizing used at East Mesa well 5-1 and Otake, Japan
Calcite in well casing	Wash with inhibited HCL	Used in Hungary and Kawerau, New Zealand
Silica in flow control equipment and heat exchangers	Wash with ammonia bifluoride	Acidizing, used in Hveragerdi, Iceland
Silica in borehole	Pump NaOH solution in to the well	Used at Matsukawa, Japan
Calcite in borehole	Reaming or re-drilling	Used in New Zealand Hungary, and Mexico
Mixed scales in turbine components	Spaced in heavy diesel oils	Used at Larderello, Italy
Mixed scales in heat exchanger tubing and piping	Cavitation descaling	-
Calcite scales (test probe)	Application of thermal shock	-

7. OPTIMIZED OPERATION WITH REGARD TO SILICA SCALING

Silica (SiO_2) is found in most geothermal fluids in different concentrations, but is more common in high temperature fields. The silica limit temperature is the temperature below which the silica dissolved in geothermal fluid may be expected to precipitate and deposit in the plant equipment or the reinjection well. An estimate of that temperature was obtained using the solubility curve for quartz and amorphous silica. The concentration of dissolved silica in the liquid part of the geothermal fluid increases as the water continues boiling in the well to the separator. Even if the water passes the amorphous silica saturation curve (Figure 16), the precipitation of silica can be delayed by changing the polymerization kinetics with pH adjustment (Thórhallsson, 2006). Little can be done to control silica deposition except to operate the system so that the geothermal fluid temperature is maintained above that which would cause precipitation. The most widely used formula for the quartz geothermometer (Fournier and Potter, 1982) to indicate the reservoir condition is:

$$t(°C) = -42.198 + 2.883 \times 10^{-1} - S^1 - 3.668 \times 10^{-4}S^2 + 3.1665 \times 10^{-7}S^3 + 77.034\ logS$$

where t = Temperature (°C);
        S = Silica concentration (mg/kg).

When the solubility of amorphous silica at the vapour pressure of the solution ranges from 0 to 250°C, the equation is given by (Fournier and Rowe, 1977):

$$\log C = -\frac{731}{T} + 4.52$$

where C = Silica concentration (mg/kg);
        T = Absolute temperature (°K).

If the plant has to operate below the safe region (Figure 16), the composition must be adjusted to control silica precipitation. Some control can be achieved through pH control. The strong relationship between pH and precipitation rate of amorphous silica from a "supersaturated" solution was observed in the Fushima field in Kyushu, Japan. It was observed that even though the acidic water discharged from well C (pH=3.9) had the highest silica concentration, it generated relatively small amounts of silica-rich scale. However, the neutral pH water, containing only moderate amounts of silica (from well F), continuously precipitated amorphous silica from both upstream and downstream sections of the test equipment. It was concluded that in the Fushima waters, the pH controls the precipitation rate of amorphous silica more than the degree of supersaturation (Grassiani, 2000). In another case study, a delay of 200min was observed with a decrease of pH from 6 to 5 in the Broadlands fields, New Zealand. Polymerization can be delayed with an addition of HCl or H_2SO_4.
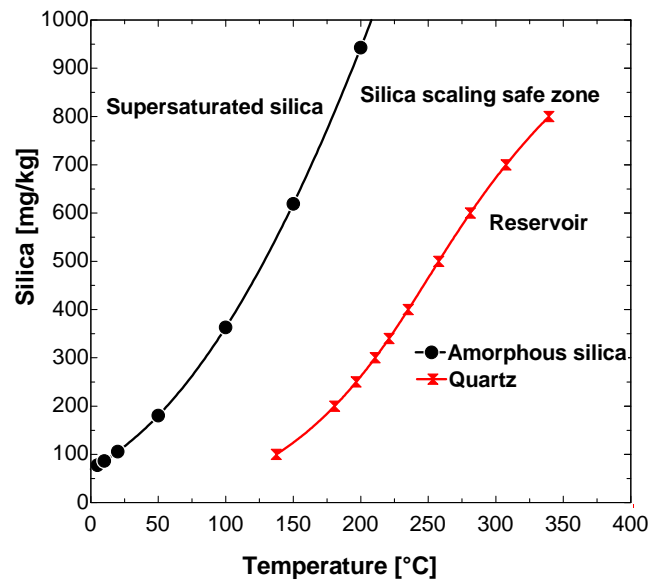
FIGURE 16: Silica scaling limiting curve

The increase of pH upstream of the heat exchanger could, however, result in the corrosion of the heat exchangers and other accessories. A rough cost analysis shows that acidification by HCl will add less than 2 mils/kWh to the cost of energy, indicating that the method will likely prove economically feasible as well. Also, experimental evidence now exists that acidification delays the formation and stabilizes the colloidal suspension of silica in the cooled brine. Thus, the plugging of reinjection wells by normally occurring suspended solids might be avoided (Kestin et al., 1980).

8. PLANT SAFETY PRACTICES

Occupational health safety issues during the operation of geothermal power generation include non-condensable gases, confined space, heat, noise, and hydrocarbon fluid (IFC, 2007). The following need to be addressed:

- Occupational exposure to geothermal gases, mainly hydrogen sulphide gas during non-routine release of geothermal fluid (for example, pipe line failures) and maintenance work in confined

spaces such as pipe lines, turbine, and condensers. The significance of the hydrogen sulphide hazard may vary depending on the location and geological formation particular to the facility.

- Confined spaces in geothermal and any other industry sectors are potentially fatal. Confined space entry by workers and the potential for accidents may vary among geothermal facilities depending on design, site equipment, and the presence of geothermal fluids. Specific and unique areas for confined space entry may include the turbine, condenser, and cooling water tower (during maintenance activity), and monitoring equipment sheds (during sampling). Geothermal power facilities should develop confined space entry procedures.

- Occupational exposure to heat occurs during construction activity and during operation and maintenance of pipes, wells and related hot equipment. Non-routine exposures include potential blow-out accidents during malfunctions of the steam contaminants and transport installations. Recommended prevention and control measures to address heat exposure include:

- Reduce the time required for work in elevated temperature environments and ensuring access to drinking water:
  - Shielding surface where workers come in close contact with hot equipment, pipes etc.
  - Use personal protective equipment (PPE) as appropriate, including insulated gloves and shoes;
  - Implement appropriate procedures during maintenance work.

- Noise sources are mainly related to wells, steam flashing and venting. Other sources include equipment related to pumping facilities, turbines, and temporary pipe flashing activity. Temporary levels may exceed 100 dBa during certain drilling and steam venting activity. Noise abatement technology includes the use of rock mufflers and sound insulation, in addition to silencers on equipment in the steam processing facility.

- Safety in isopentane handling. Isopentane is a colourless liquid with a gasoline-like odour. It is highly flammable in liquid and vapour states and also capable of causing flash fires. Vapour may accumulate in low or confined areas, travel a considerable distance to a source of ignition and flash back. In case of contact with isopentane, immediately flush with plenty of water the eye or body part which came into contact. It is important to use isopentane with caution.

9. DISCUSSION OF RESULTS

Energy analysis

An energy analysis was done for high-temperature wells LA 3 and LA 6. The EES programme is presented in Appendix I. Comparison of power generation decline was done for wellhead pressure at 12.5 bars to 5.6 bars. The results of the output power from the GCCU unit for the steam turbine and the organic turbine are indicated in Table 6, but the modules and the T-S diagrams for isopentane are given in Appendix II.

From the results it can be seen that the gross net power output has declined. Much of the decline is with the power output of the steam turbine. But the output of the organic turbine did not show a decline due to an increase in mass flow. The output temperatures from the GCCU shell and tube vaporizer are shown in Figures 17 and 18. The output temperature from the vaporizer is greater when operating the plant at the lower pressure of 5.5 bars than at 12.5 bars, for about 3°C. The decline of the isopentane temperature at the vaporizer outlet is due to the decrease in mass flow in the wells with pressure increase.

TABLE 6: Power generation decline

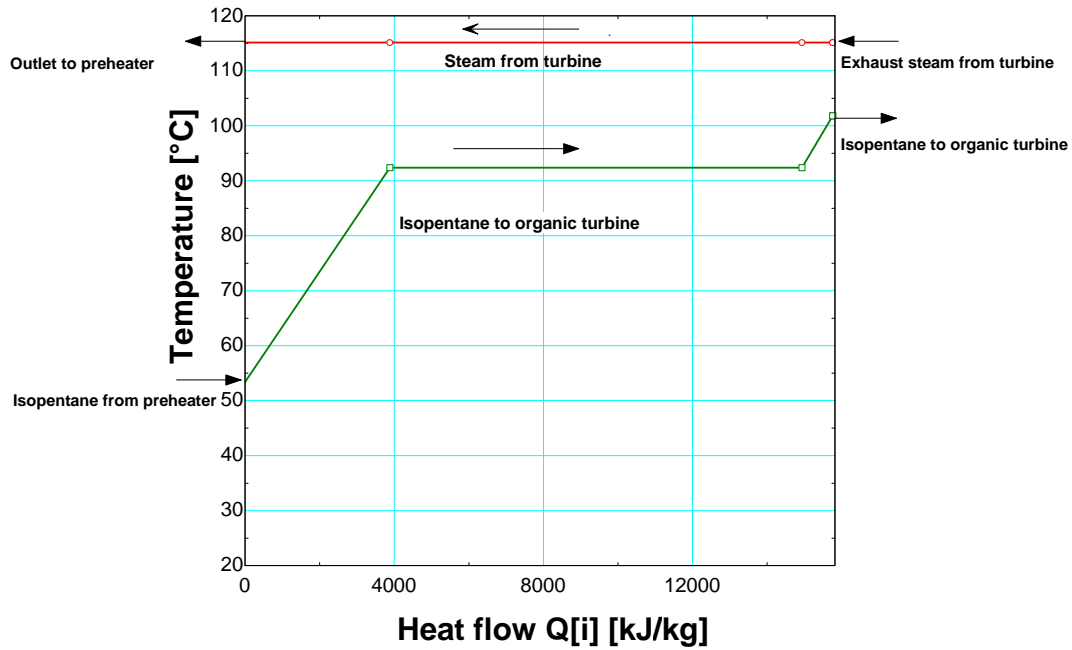| Well head pressure LA-3 (bar)	Well head pressure LA-6 (bar)	Enthalpy LA-3 (kJ/kg)	Enthalpy LA-6 (kJ/kg)	Temp. sep. (°C)	Steam mass flow to turbine (kg/s)	Power from steam turbine (kW)	Power from organic turbine (kW)	Total power (kW)
5.6	5.5	1725	1655	156	10.08	946.3	2468	3414
12.5	13.15	1730	1655	190	7.226	1780	2371	4151

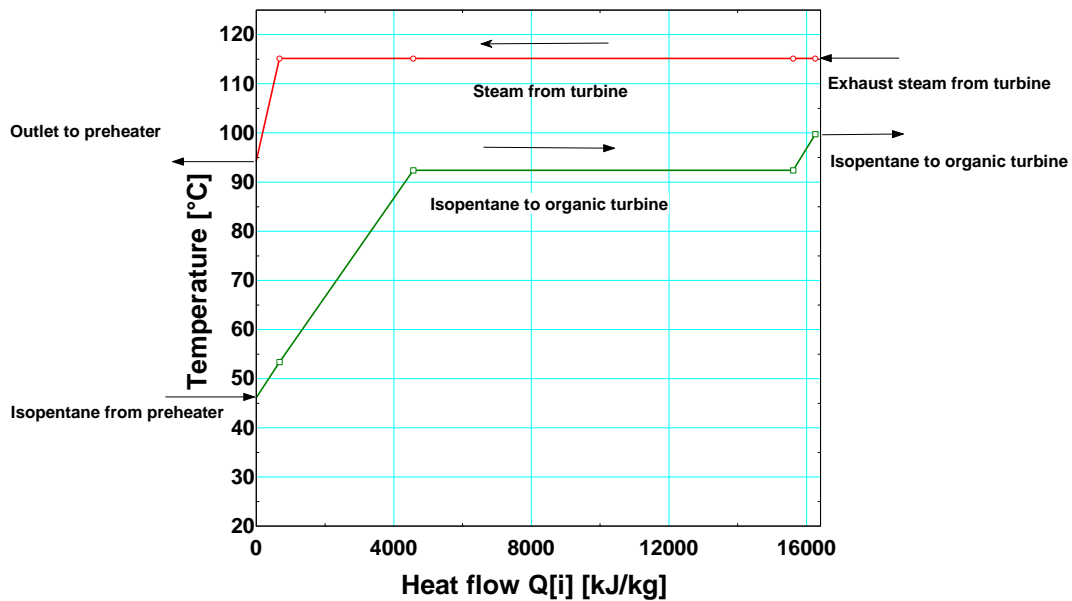FIGURE 17: Flow in GCCU vaporizer at 5.6 bar pressure wellhead pressure

FIGURE 18: Flow in GCCU vaporizer at 12.5 bar wellhead pressure

Operation of the plant at higher mass flow with lower pressure does not have much effect on the power output of the organic turbine but has led to a big decrease in the steam turbine output. This can be seen on the pressure vs. power curve result from EES in Figure 19.

The steam for the steam turbine is supplied from high-temperature wells LA-3 and LA-6 located at different distances from the power plant. The steam from the two wells enters the GCCU unit in a common pipe line. LA-6 is located 870 m from the power plant but LA-3 is located about 380 m from the power plant. The steam pipe lines are connected at about 250 m from the power plant. There was a large pressure drop in the LA-6 steam pipe line as the flow increased. Pressure drop in the transmission pipe increased with an increase in the flowrate. Thus, the wells had to be operated at different pressures to get a similar pressure supply. The pressure drop was calculated for different

wellhead pressures. The results indicate that LA-6 cannot be operated at less than 7.5 bars for parallel operation. This is indicated in Figure 20.

Operating the plant at low temperatures can create silica scaling problems. A flashing calculation was done for the four wells (Figure 21) and emphasis was made here on wells LA-3 and LA-6 as they are the current production wells. The medium-temperature wells, LA-4 and LA-8, can be used at lower temperatures than the high-temperature wells.

The operation of the plant without silica scaling is at the limits of the amorphous silica solubility line. Figure 22 indicates the flow of the wells to be close to silica super saturation. The limit for Wells LA-3 and LA-6 is above 182°C. But the current operation of the plant is at about156°C at the steam separator (see Table 6), limited by the drawdown of wellhead pressure. This indicates that the possibility of using the separated water at the wellhead separators for the OEC unit could cause further scaling in the pipes and the reinjection well.

FIGURE 19: Power output vs. wellhead pressure
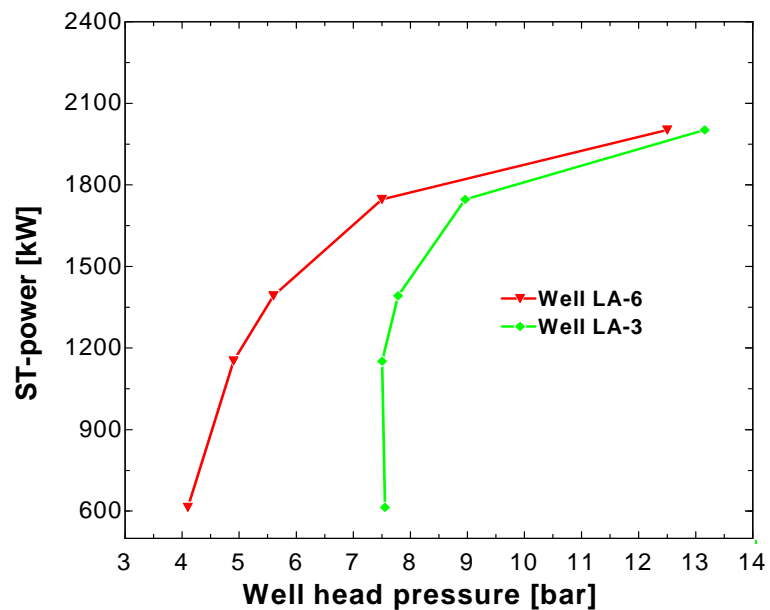
FIGURE 20: Parallel operation of wells

10. CONCLUSIONS AND RECOMMENDATIONS

The purpose of this project was to analyze the problems in the Aluto Langano power plant and suggest solutions using the experience of others. An energy analysis was done to analyze the effects of a decline in wellhead pressure. The following points have to be stressed:

- Some investment has to be made for modification in design and installation of instruments to attain trouble free operation.
- Usage of separated water for further power generation in the OEC unit could cause scaling on surface equipment and in the reinjection well.
- Current reinjection conditions are in the silica super saturation zone and require the addition of chemicals to slow precipitation.
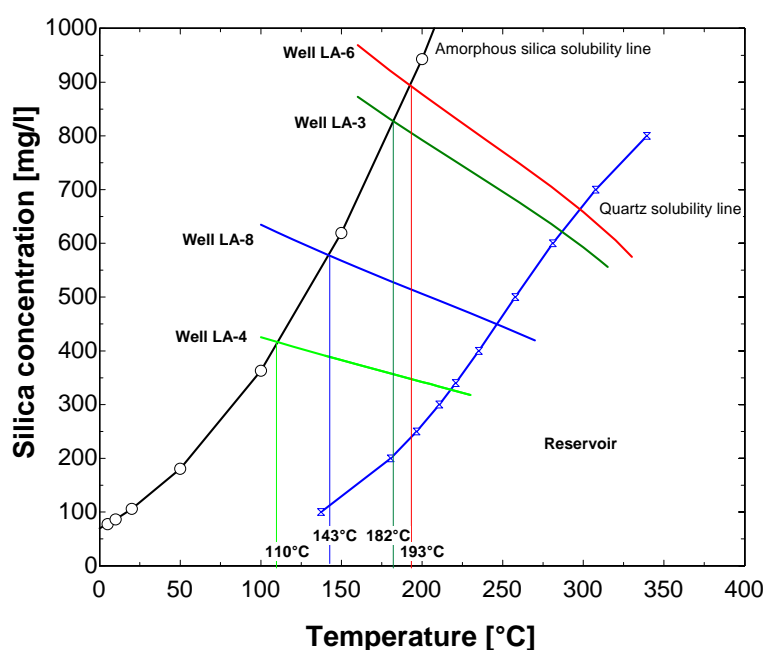- Further investigation is needed to determine flow and the chemical contents of the wells as most data taken for analysis were old.

FIGURE 21: Flashing curve for wells LA-3 LA-4,
LA-6 and LA-8
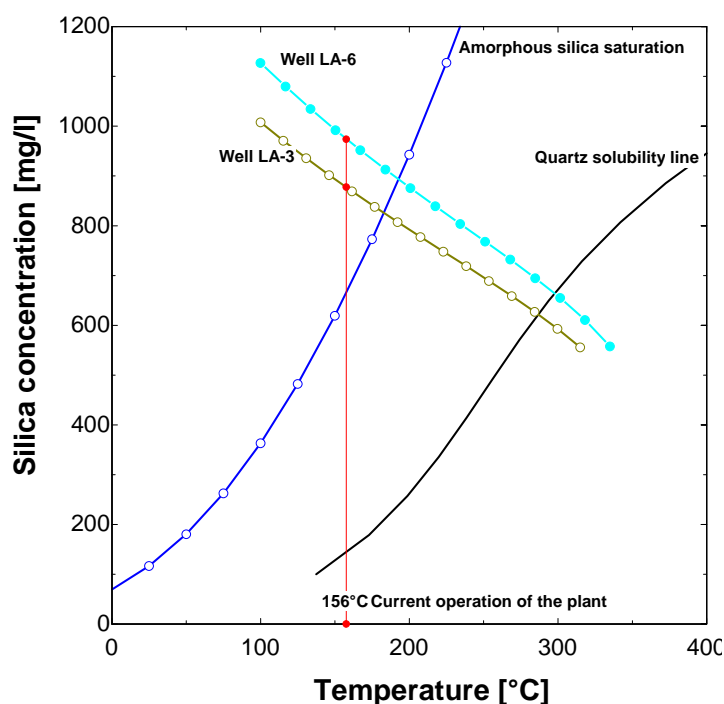
FIGURE 22: Current well operation

ACKNOWLEDGEMENTS

REFERENCES

Amdeberhan,Y., 2006: Well testing and reservoir engineering studies at Aluto Langano & Tendaho geothermal fields, Ethiopia. *First International Conference on Geothermal Energy in the East African Rift Region, ARGeo C-1, Abstracts,* 34.

Benoit, D., 2006: *Preliminary assessment of wells, June 29 – Dec. 11, 2006.* EEPCo, unpublished report, 34 pp.

Cengel, Y.A., and Turner, R.H., 2001: *Fundamentals of thermal-fluid sciences.* University of Nevada, Reno, 1200 pp.

Deutscher, S.B., Ross, D.M., Quong, R., and Harrar, J.E., 1980: *Study of dissolution of geothermal scale.* Lawrence Livermore Laboratory, University of California, 20 pp.

El-Wakil, M.M., 1984: *Power plant technology.* McGraw-Hill, Inc., USA, 859 pp.

F-Chart Software, 2004: *EES, engineering equation solver.* F-Chart Software, website, http://www.fchart.com/ees/ees.shtml.

Fournier, R.O., and Potter, R.W., 1982: An equation correlating the solubility of quartz in water from 25° to 900°C at pressures up to 10,000 bars. *Geochim. Cosmochim Acta, 46,* 1969-1973.

Fournier, R.O., and Rowe, J.J., 1977: The solubility of amorphous silica in water at high temperatures and high pressures. *Am. Min., 62,* 1052-1056.

Grassiani, M. 2000: Siliceous scaling aspects of geothermal power generation using brine cycle heat recovery. *Proceedings of the World Geothermal Conference 2000, Kyushu-Tohoku, Japan,* 3167-3171.

IFC, 2007: Environmental, health, and safety guide lines. IFC, website: http://www.ifc.org/ifcext/enviro.nsf/AttachmentsByTitle/gui_EHSGuidelines2007_GeothermalPower Gen/$FILE/Final+-+Geothermal+Power+Generation.pdf

Kestin, J., DiPippo, R., Khalifa, H.E., and Ryley, J. (editors), 1980: *Sourcebook on the production of electricity from geothermal energy.* U.S. Depmt. of Energy, Washington, D.C., 997 pp.

Ketema, T., and Solomon, K., 1983: *Challenges and initiatives to be taken to develop geothermal resources in Ethiopia.* Geological Survey of Ethiopia, unpublished report, Addis Ababa.

Koutsoukos, P., and Andritsos, N., 2002: Corrosion in geothermal plants. *Proceedings of International Course on District Heating, Agricultural and Agro-industrial Uses of Geothermal Energy, Thessaloniki, September,* 190-201.

Morris, W.F., and Stephens, F.B., 1981: *Strategies for steam handling and H_2S abatement at geothermal power plants in the Geysers area of northern California.* Lawrence Livermore National Lab, CA report, 72 pp.

Ormat, 2001: *Ethiopia, Aluto-Langano. The power of innovation, projects, geothermal power plants.* Ormat, website: http://www.ormat.com/index-project.htp.

Phillips, S.L., Mathur, A.K., and Doebler, R.E., 1977: A study of treatment methods for geothermal fluids. *SPE International Symposium on Oilfield and Geothermal Chemistry, Proceedings,* 2-8.

Robertus, R.J. Sullivan, R.G., Pool, K.H., Shannon, D.W., Kindle, C.H., and Pierce D.D., 1984: *Leak detectors for organic Rankin cycle power plants*: *Online manual methods.* Prepared for U.S. Department of Energy, report, 62 pp.

Sakuma, A., Matsuura, T., Suzuki, T., Watanabe, O., and Fukuda, M., 2006: Upgrading and life extension technology for geothermal steam turbines. *JSME Int. Jour Series B, 49-2*/186-191.

Teklemariam, M., Battaglia, S., Gianelli, G., and Ruggieri, G., 1996: Hydrothermal alteration in the Aluto-Langano geothermal field, Ethiopia. *Geothermics, 25-6, 679-702.*

Thórhallsson, S., 2006: Common problems faced in geothermal generation and how to deal with them. *Workshop for Decision Makers on Geothermal Projects in Central America 2006, San Salvador, UNU-GTP and LaGeo,* CD SC-04, 8 pp.

Thórólfsson, G., 2005: Maintenance history of a geothermal plant: Svartsengi Iceland. *Proceedings of the World Geothermal Congress 2005, Antalya, Turkey*, CD, 7 pp.

Valdez, B., Schorr, M., and Arce, A., 2006: The influence of minerals on equipment corrosion in geothermal brines. *Proceedings of International Mineral Extraction from Geothermal Brines Conference, Arizona*, 4 pp.

APPENDIX I: Part of the EES calculation model

"Balancing of pressure at wells LA-3, LA-6"
P_1=P_W1"- - - - - - -Wellhead pressure at LA-3 from Table 6"

"Adjustment of the wellhead pressure after calculating the wellhead pressure drop, P_19 calculated below"
P_2=P_19+p_drop6"- - - - - - -Wellhead pressure at LA-6 calculated"
X_w2=Quality(water,h=h_w2,P=P_W2)"- - - - - - calculated quality for LA_6 from Table 6"
h_2=Enthalpy(water,x=X_w2,p=P_2)"- - - - - - calculated enthalpy for LA_6 "

"Temperature values for four wells, LA-3, LA-6, LA-4, LA-8"
t_1=temperature(water,p=p_1,x=1)
t_2=temperature(water,p=p_w2,x=1)
t_3=temperature(water,p=p_3,x=1)
t_4=temperature(water,p=p_4,x=1)

"Well LA-3, Pressure P1, Mass flow M1, Energy and mass balance"
"values given in Table 6"
P_5=P_1
P_9=P_1

h_5=ENTHALPY(Water,p=p_1,x=1)
h_9=ENTHALPY(Water,p=p_1,x=0)

m_gas1=m_dot_1*0.023"- - - - - - gas content 2.3% in mass"

m_dot_5+m_dot_9=m_dot_1-m_gas1
m_dot_5*h_5+m_dot_9*h_9=(m_dot_1-m_gas1)*(h_1)

S_A1=Entropy(water,P=P_1,h=h_1)

T_A[0]=temperature(water,x=0,h=1550)"- - - - - - - - - - Condition in the reservoir"

S_A[0]=Entropy(water,x=0,h=1550)

T_A[1]=t_1
S_A[1]=S_A1

{Well LA-6, Pressure P2, Mass flow M2, Energy and mass balance}
"values given in Table 6"
P_6=P_2
P_10=P_2

m_dot_2=13.6316 - 0.127201*p_2"- - - - - - - - - - - Equivalent mass flow from LA-6 for the pressure P_2"
h_6=ENTHALPY(Water,p=p_2,x=1)
h_10=ENTHALPY(Water,p=p_2,x=0)

m_gas2=m_dot_2*0.026"- - - - - - gas content 2.6% in mass"
m_dot_6+m_dot_10=(m_dot_2-m_gas2)
m_dot_6*h_6+m_dot_10*h_10=((m_dot_2-m_gas2)*h_2)
m_gas_19=m_gas1+m_gas2"- - - - - -Total non condensable gas content at inlet of turbine"

"Well LA-4, Pressure P3, Mass flow M3, Energy and mass balance"
"values given in Table 6"
P_7=P_3
P_11=P_3

h_7=ENTHALPY(Water,p=p_3,x=1)
h_11=ENTHALPY(Water,p=p_3,x=0)

m_dot_7+m_dot_11=m_dot_3
m_dot_7*h_7=m_dot_3*h_3-m_dot_11*h_11

"Brine Pump, LA-4"
P_BPPower_4=15[kW]*PUMPON_4"- - - - - - - Power on off"
eta_BPump=0.85
eta_Bmotor=0.90
rho_11=Density(water,P=P_11,x=0)

delta_p11=pump(P_BPPower_4,eta_Bmotor,eta_Bpump,m_dot_3,rho_11)

P_13=Delta_p11+P_11

"Well LA-8, Pressure P4, Mass flow M4, Energy and mass balance"
P_8=P_4
P_12=P_4

h_8=ENTHALPY(Water,p=p_4,x=1)
h_12=ENTHALPY(Water,p=p_4,x=0)

m_dot_8+m_dot_12=m_dot_4
m_dot_8*h_8=m_dot_4*h_4-m_dot_12*h_12

"Brine Pump, LA-8"
P_BPPower_8=22*PUMPON_8 "- - - - - - - Power on off condition"
rho_12=Density(water,P=P_12,x=0)

P_14=Delta_p12+P_12

delta_p12=pump(P_BPPower_8,eta_Bmotor,eta_Bpump,m_dot_4,rho_12)

{GCCU Steam turbine Inlet, pressure drop calculation}
"Pressure drop from LA3 to connection point to LA6"
rho_5=Density(steam,P=P_1,x=1)
Ds_5=0.2101"- - - - - - - - Nominal diameter of pipe"
DN_5=0.200"- - - - - - - - Internal diameter of pipe"
head_5=-10"- - - - -Elevation difference"
L_p5=130"- - - - - - - - - - Length of pipe"
L_eq5=L_p5+L_eb5+L_ev5+L_ej5"Equivalent length of bends, valves and junctions"
L_eb5=6*20*DN_5
L_ev5=2*10*DN_5
L_ej5=0
e=0.046/1000

mu_5=VISCOSITY(Steam,X=1,P=P_1)

m_dot_5=rho_5*v_5*((Ds_5)^2)*PI/4

p_drop5=rho_5*g#*(head_5+h_floss5)/100000

h_floss5=f_5*(L_eq5*v_5^2)/(Ds_5*2*g#)

1/sqrt(f_5)=-2*log10(((e/Ds_5)/3.7)+2.51/(Re_5*sqrt(f_5)))

Re_5=rho_5*v_5*(Ds_5/mu_5)

"Pressure drop from LA6 to connection point to LA3"
rho_6=Density(steam,P=P_19,x=1)
Ds_6=0.2101"- - - - - - - - Nominal diameter of pipe"
DN_6=0.200"- - - - - - - - Internal diameter of pipe"
head_6=-50.1"- - - - -Elevation difference"

L_p6=620"- - - - - - - - - - Length of pipe"
L_eq6=L_p6+L_eb6+L_ev6+L_ej6 "Equivalent length of bends, valves and junctions"
L_eb6=22*20*DN_6
L_ev6=2*10*DN_6
L_ej6=2*20*DN_6

mu_6=VISCOSITY(Steam,X=1,P=P_2)

m_dot_6=rho_6*v_6*((Ds_6)^2)*PI/4

p_drop6=rho_6*g#*(head_6+h_floss6)/100000

h_floss6=f_6*(L_eq6*v_6^2)/(Ds_6*2*g#)

1/sqrt(f_6)=-2*log10(((e/Ds_6)/3.7)+2.51/(Re_6*sqrt(f_6)))

Re_6=rho_6*v_6*(Ds_6/mu_6)

m_dot_19=m_dot_5+m_dot_6
h_19=(m_dot_6*h_6+m_dot_5*h_5)/m_dot_19

P_19=P_5-p_drop5

{Flash Tank, Energy and mass balance}

h_14=ENTHALPY(Water,P=P_14,x=0)
h_13=ENTHALPY(Water,P=P_13,x=0)

"Mass balance and energy balance in flash tank"
m_dot_15=m_dot_9+m_dot_10+m_dot_11+m_dot_12" - - - - - - - - - - - -Separated water from LA-3, LA-6, LA-4, LA-8 "
m_dot_15*h_15=m_dot_9*h_9+m_dot_10*h_10+m_dot_11*h_11+m_dot_12*h_12
m_dot_15*t_15=m_dot_9*t_1+m_dot_10*t_2+m_dot_11*t_3+m_dot_12*t_4
P_Ftank=5[bar] "- - - - - - - - - Pressure in flash tank in bar"
h_16=enthalpy(Steam,P=P_Ftank,x=1)
h_18=enthalpy(Steam,P=P_Ftank,x=0)

m_dot_15=m_dot_16+m_dot_18
m_dot_15*h_15=m_dot_16*h_16+m_dot_18*h_18
m_dot_17=m_dot_16+m_dot_7+m_dot_8

"Pressure drop from connection point to Power plant"
rho_19=Density(steam,P=P_19,x=1)
Ds_19=0.312"- - - - - - - - Nominal diameter of pipe"
DN_19=0.300"- - - - - - - Internal diameter of pipe"
head_19=-5"- - - - - - - - -Elevation difference"

L_p19=250"- - - - - - - - - Length of pipe"
L_eq19=L_p19+L_eb19+L_ev19+L_ej19"Equivalent length of bends, valves and junctions"
L_eb19=16*20*DN_19
L_ev19=1*10*DN_19
L_ej19=1*20*DN_19

mu_19=VISCOSITY(Steam,X=1,P=P_19)

m_dot_19=rho_19*v_19*((Ds_19)^2)*PI/4

p_drop19=rho_19*g#*(head_19+h_floss19)/100000

h_floss19=f_19*(L_eq19*v_19^2)/(Ds_19*2*g#)

1/sqrt(f_19)=-2*log10(((e/Ds_19)/3.7)+2.51/(Re_19*sqrt(f_19)))

Re_19=rho_19*v_19*(Ds_19/mu_19)

T_A[2]=T_1
S_A[2]=Entropy(water,X=1,t=t_1)

T_A[3]=t_STin
S_A[3]=S_STin

"GCCU steam turbine outlet"
P_STin=P_19-p_drop19
m_dot_STin=m_dot_19
H_STin=h_19   {ENTHALPY(Steam;x=1;P=p_STin)}
t_STin=temperature(Water,P=P_STin,h=H_STin)

H_gas_STin=ENTHALPY(CarbonDioxide,T=T_STin,P=P_STin)
H_gas_STout=ENTHALPY(CarbonDioxide,T=T_STout,P=P_STout)
P_STgaspower=m_gas_19*(H_gas_STin-H_gas_STout)*0.95

S_STin=ENTROPY(Steam,h=H_STin,P=p_STin)
S_STout=ENTROPY(Steam,h=H_STout,P=p_STout)

eta_ST=0.80   "- - - - - - - -Isentropic efficiency"
H_STout_s=Enthalpy(Steam,P=p_STout,S=S_STin)
eta_ST=(H_STin-H_STout)/(H_STin-H_STout_s)

P_STout=1.7   "- - - - - - - - -Assumed Pressure outlet at the turbine"
X_STout=Quality(Water,P=P_STout,H=H_STout)
P_STpower=(m_dot_STin*(H_STin-H_STout)+P_STgaspower)*0.90   "- - - - - - - - - - - --
Assumed generator Efficiency"
P_Tpower=P_STpower+P_OTpower
t_STout=temperature(Steam,P=p_STout,H=H_STout)

T_A[4]=T_STout
S_A[4]=S_STout
T_A[5]=T_STout
S_A[5]=Entropy(water,X=0,t=T_STout)

"Organic turbine output"
P_OTin= 6.1"- - - - -Assumed isopentane inlet pressure bar"
t_Vout=t_OTin

P_OTout=1.1"- - - - -Assumed outlet pressure in bar"
m_dot_IP=140800/3600"- - - - - - - - - Average flow of Isopentane in Kg/s"

H_OTout=ENTHALPY(ISOPENTANE,t=t_OTout,P=p_OTout)
H_OTin=ENTHALPY(ISOPENTANE,t=t_OTin,P=p_OTin)
S_OTin=ENTROPY(ISOPENTANE,h=H_OTin,P=p_OTin)

eta_OT=0.86
H_OTout_s=Enthalpy(Isopentane,P=p_OTout,S=S_OTin)
eta_OT=(H_OTin-H_OTout)/(H_OTin-H_OTout_s)

t_OTout=temperature(ISOPENTANE,S=S_OTout,P=p_OTout)
P_OTpower=m_dot_IP*(H_OTin-H_OTout)*0.90"- - - - - - - - - - - - Power output of Organic turbine
with assumed generator Efficiency 92%"

T_Aiso[5]=t_OTout
S_Aiso[5]=S_OTout

"Isopentane Cooling and Saturation in Condenser"
H_idew=ENTHALPY(ISOPENTANE,x=1,P=P_OTout)
t_idew=Temperature(ISOPENTANE,H=H_idew,P=P_OTout)

S_idew=ENTROPY(ISOPENTANE,t=t_idew,H=H_idew)

T_Aiso[6]=t_idew
S_Aiso[6]=S_idew

P_COout=P_OTout
t_COin=t_OTout
t_COout=t_idew
S_COout=ENTROPY(ISOPENTANE,t=t_COout,X=0)
H_COout=ENTHALPY(ISOPENTANE,t=t_COout,S=S_COout)
T_Aiso[0]=t_COout
S_Aiso[0]=S_COout

T_Aiso[7]=t_COout
S_Aiso[7]=S_COout

{Isopentane cycle pump}

P_CPin=P_COout
S_CPin=S_COout
S_CPin=S_CPout
P_CPout=6.1" Average pumping pressure of cycle pump in bar"
H_CPin=ENTHALPY(ISOPENTANE,P=P_CPin,S=S_CPin)
H_CPout=ENTHALPY(ISOPENTANE,P=P_CPout,S=S_CPout)
t_CPout=temperature(ISOPENTANE,S=S_CPout,H=H_CPout)

t_CPout[1,7]=t_CPout
S_CPout[1,8]=S_CPout

"Isopentane Preheater"
U_p=0.8"- - - - - - - - - -Assumed overall heat transfer coefficient"
H_Prein=H_CPout
A_p=55 "- - - - - - - - - -Assumed area of preheater square meter"

P_Preout=P_CPout

P_Bprein=3
t_Prein=t_CPout

"Energy balance in the preheater"
Q_Pre=m_dot_IP*(H_Preout-H_Prein)

t_bprein=t_bvout
H_BPreout=Enthalpy(water,P=P_BPrein,t=t_BPreout)

S_Preout=Entropy(Isopentane,t=t_Preout,P=P_Preout)

Q_Pre=Q_BPre

Q_BPre=m_dot_STin*(H_BPrein-H_BPreout)
LMTD_p=LMTD(t_Bprein,t_Bpreout,t_Prein,t_Preout)
Q_pre=U_p*A_p*LMTD_p

H_BPrein=Enthalpy(water,P=P_BPrein,t=t_Bprein)

H_Preout=Enthalpy(Isopentane,t=t_Preout,P=P_Preout)

T_Aiso[1]=t_preout
S_Aiso[1]=S_Preout

S_Bpreout=Entropy(water,t=t_BPreout,h=H_BPreout)

T_A[7]=t_Bpreout
S_A[7]=S_Bpreout

{Isopentane Vaporizer}

U_vap=1.4"- - - - - - - - - - -Assumed overall heat transfer coefficient"
A_vap=451"- - - - - - - - - - -Assumed area of Vaporizer square meter"
P_Vin=P_preout
m_vin=m_dot_IP

t_vin=t_preout

m_bvin=m_dot_STin-(m_dot_stin*0.03)"Steam loss with the release of NCG gas"
P_bvin=P_STout
t_Bvin=t_STout
x_bvin=X_STout

H_Bvin=Enthalpy(Water,P=P_bvin,T=t_Bvin)
H_Bvout=Enthalpy(Water,t=t_Bvout,P=P_bvin)

S_Vout=Entropy(Isopentane,t=t_Vout,P=P_Vin)
H_Vout=Enthalpy(Isopentane,t=t_Vout,P=P_Vin)

T_Aiso[2]=Temperature(isopentane,x=0,p=6)
S_Aiso[2]=Entropy(isopentane,x=0,p=6)

T_Aiso[3]=Temperature(isopentane,x=1,p=6)
S_Aiso[3]=Entropy(isopentane,x=1,p=6)

T_Aiso[4]=t_vout
S_Aiso[4]=S_Vout

S_Bvout=Entropy(water,t=t_bvout,h=h_bvout)
T_A[6]=t_Bvout
S_A[6]=S_Bvout
Call   Vaporizor(m_bvin,t_bvin,x_bvin,m_vin,t_vin,p_vin,U_vap,A_vap   :
case,t_vout,t_bvout,Q[0],Q[1],Q[2],Q[3],Q[4],tiso[0],tiso[1],tiso[2],tiso[3],tiso[4],tbri[0],tbri[1],tbri[2
],tbri[3],tbri[4])

APPENDIX II: Part of the EES model results at 12.5 and 5.6 bars
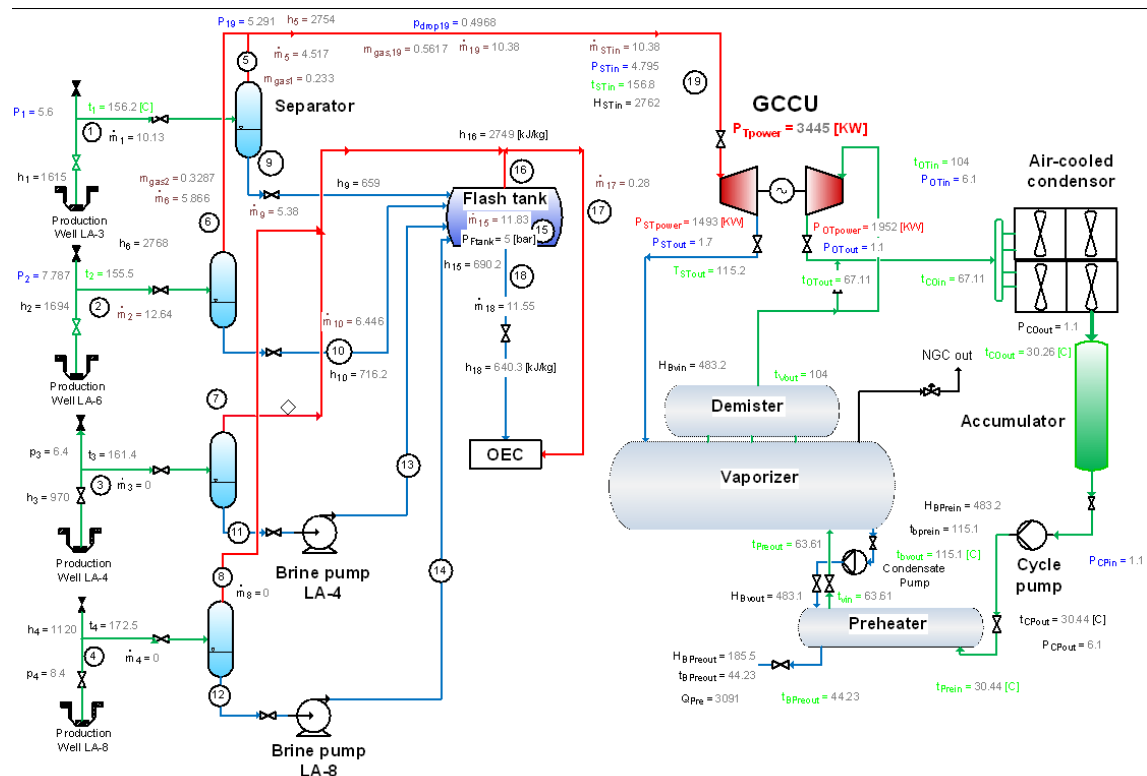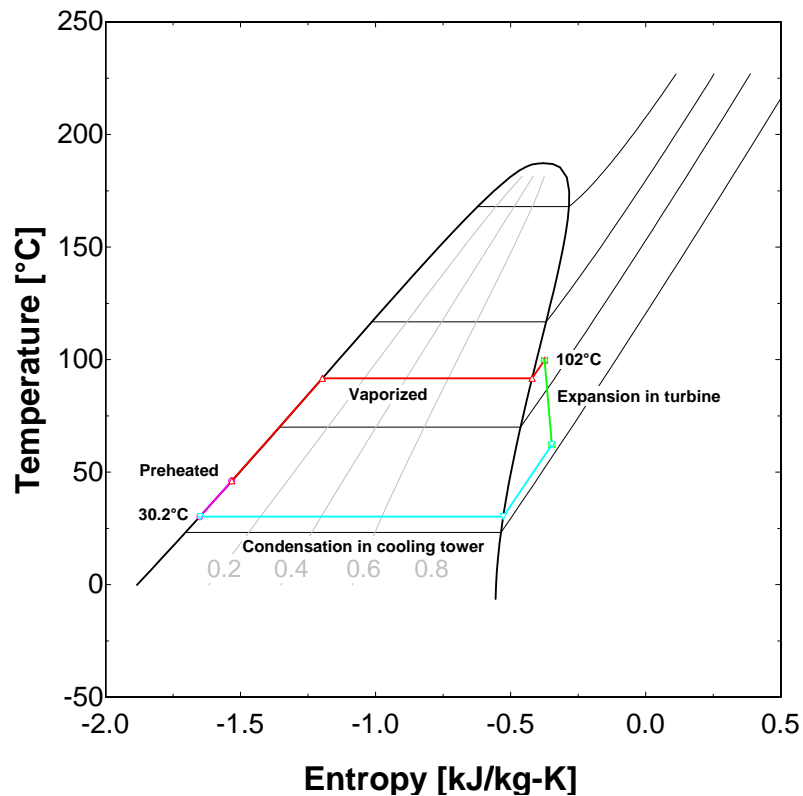

FIGURE 1: Model at 5.6 bars

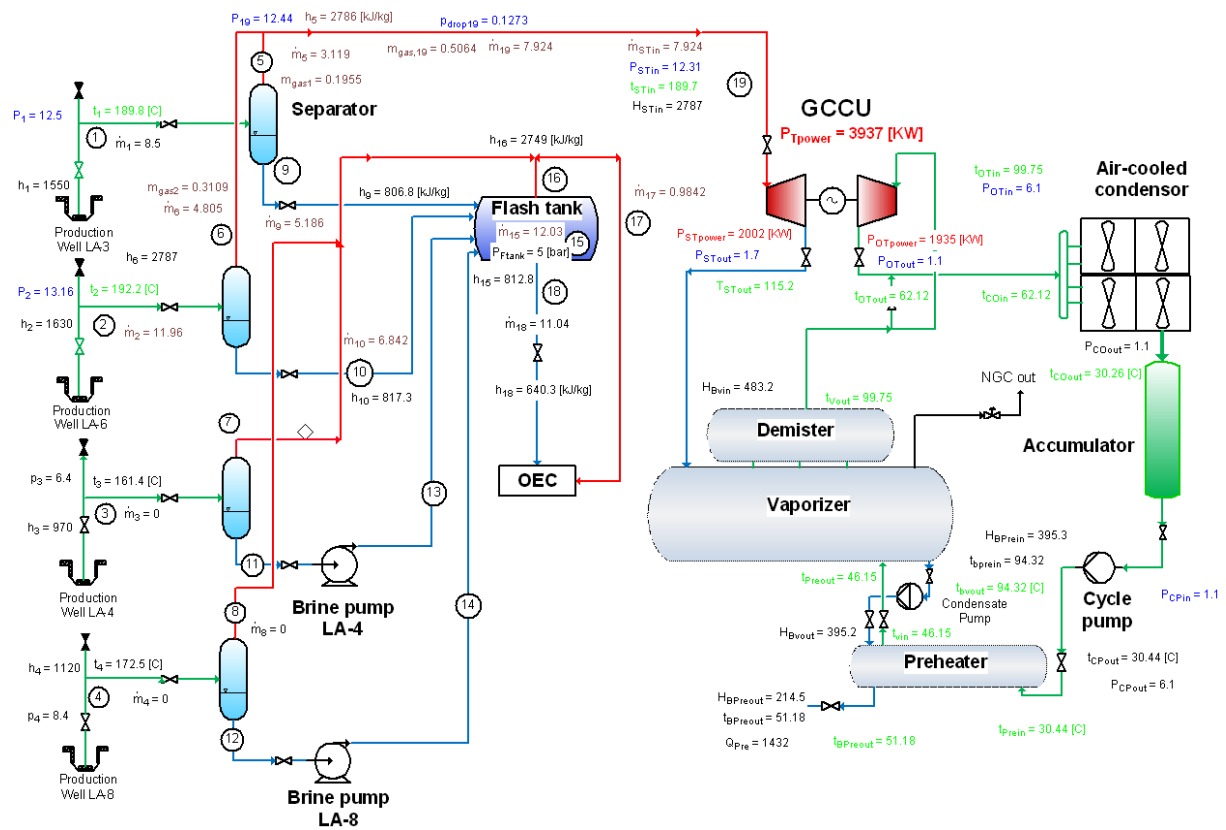FIGURE 2: T-S diagram for isopentane at 5.6 bars wellhead pressure
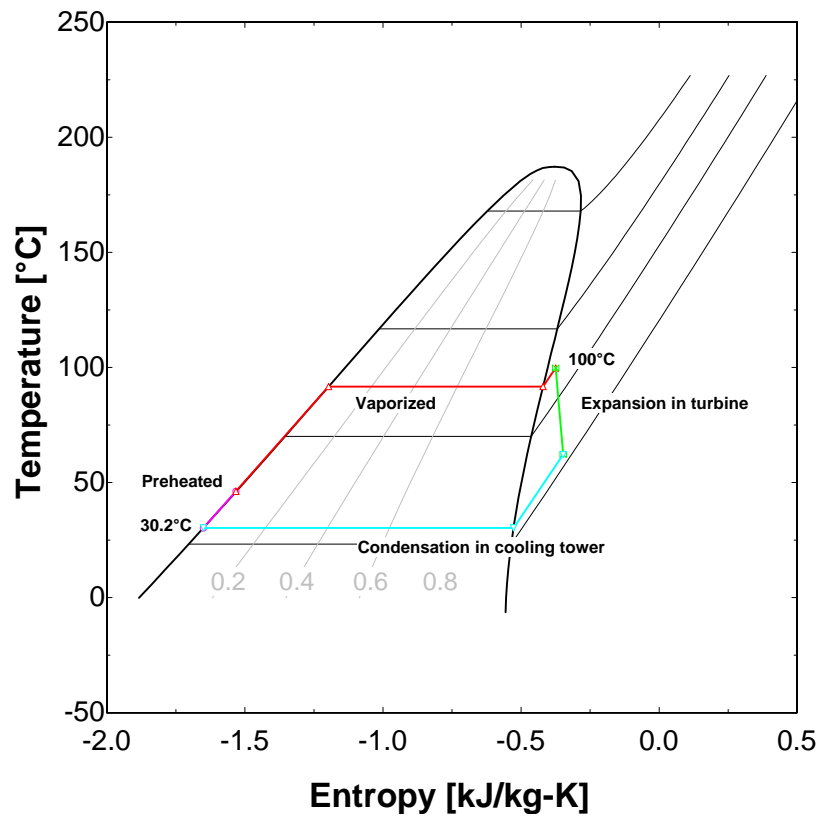
FIGURE 3: Model at 12.5 bars

FIGURE 4: T-S diagram for isopentane at 12.5 bars wellhead pressure